Land-atmosphere coupling strength for locally generated convection regimes at the ARM SGP site: Comparisons among Observations, Reanalysis, and Model Simulations

Cheng Tao (tao4@llnl.gov) and Yunyan Zhang

Lawrence Livermore National Laboratory

ECRP DOE Early Career Research Program

Motivation

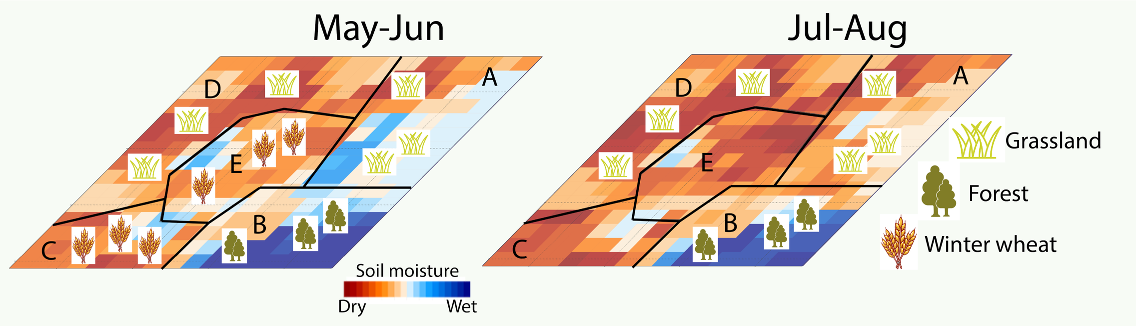

A discrepancy exists between models and observations on the strength of L-A coupling at the ARM SGP site. Using 10-yr warm season observational data, we found that:

- Surface evaporation is relatively more important on local convective events.
- In clear-sky regime, the control of the land surface on the evolution of PBL is dependent on the vegetation leaf area index (LAI).
- With similar soil conditions, the forest region shows a much higher cloud fraction on fair-weather shallow cumulus days than grassland region.

In this study, we further investigate the L-A coupling in locally-generated convection regimes (Zhang and Klein, 2010) by comparing model simulations with long-term in-situ observations. The objective is to make diagnosis on model deficiencies and to attribute model biases to parameterized processes.

Data

Observations at the ARM SGP site

- ARM continuous forcing data (VARANAL): large-scale forcing, surface heat flux, precipitation, water budget and energy budget components, etc.
- ARM Best Estimate (ARMBE): vertical profile of cloud fraction
- 915-MHz Radar Wind Profiler (RWP): convective mixed layer top
- Balloon-Borne Sounding System (SONDE): vertical profiles of temperature and humidity

NARR (North American Regional Reanalysis)

- 3-h temporal and 32-km horizontal resolution
- Developed with Eta model (2003 version) and 3DVAR technique
- Coupled to the Noah land surface model
- Derives latent heating profiles from precipitation analyses and from this forcing produces the NARR precipitation

CAPT (Cloud-Associated Parameterizations Testbed)

- A technique to diagnose the contribution of fast physical processes in the atmosphere to long-term errors in climate simulations
- CAM5.1/CLM4 coupled system run in a controlled hindcast configuration
- The 3D fields of atmospheric prognostic dynamic and thermodynamic state variables from ERA-Interim Reanalysis were initialized at the beginning of each simulation day.

Estimation of Z_i from RWP

Dataset

- The 915-MHz Radar Wind Profiler (RWP) moments files (sgp915rwpwindmomC1.*)

Methodology (Provided by Dr. Virendra Ghate from ANL)

- The top of the PBL (the entrainment zone) is very visible because the large humidity and temperature gradient there causes a large change in index of refraction.
- The maximum value of the radar-derived refractive index parameters C_n^2 often provides a good estimate of the depth of the PBL.
- The profiler signal-to-noise ratio (SNR) at a given range is directly proportional to C_n^2. Therefore, a peak in the range-corrected SNR indicates the CBL top z_i.

$$C_n^2 = \frac{1.54 \times 10^{-13} T_0}{\alpha^2 P_t n_c A_p} \lambda^{1/3} \left(\frac{R}{\Delta R}\right)^2 \mathrm{SNR}$$

Status

- RWP-derived Z_i are now available for all the defined clear-sky days (2004-2013)
- Currently, we're working on the RWP-derived Z_i for ShCu days, with CBH from ceilometer.

Example

- The RWP-derived Z_i corresponds to the top of the convective mixed layer.

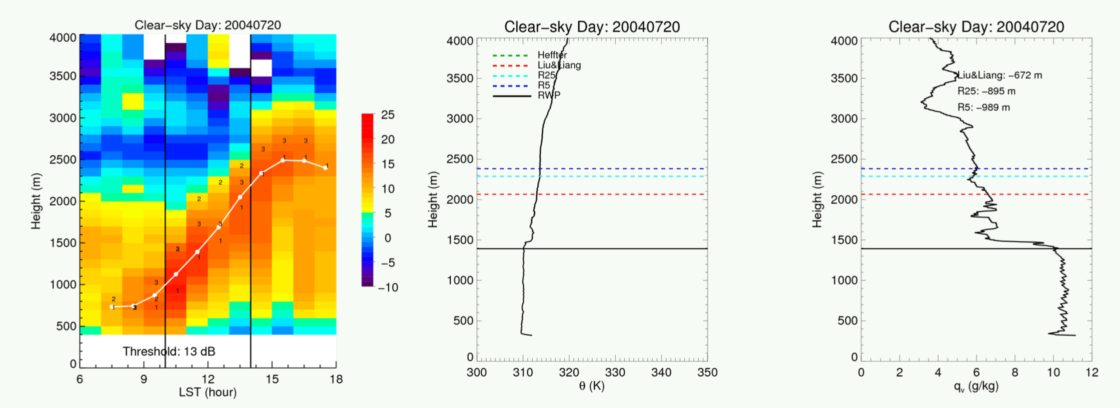

Fig. 7: (left) Time-height signal-to-noise (SNR) ratio. White dots represent the final estimation of Z_i, and number 1, 2, and 3 represents the first, second, and third guess of Z_i. (middle) Vertical profile of potential temperature. Black solid line represents the estimation of Z_i from RWP, and dashed lines represent the estimation of Z_i from SONDE. (right) Vertical profile of mixing ratio. The difference between the RWP-derived Z_i and SONDE-derived Z_i are denoted.

General comparison

Daily Mean Water Budget Components

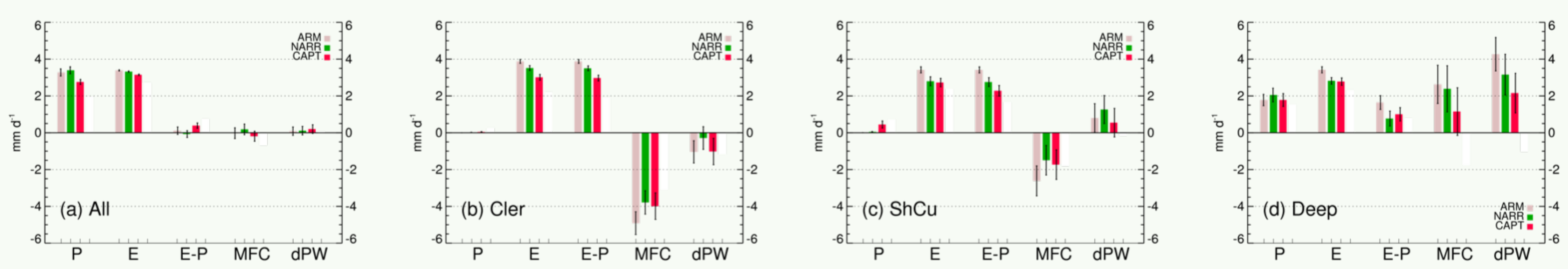

Fig. 1: Warm season (MJJA) daily-mean values of water budget components. The width of the lines indicate two standard errors.

Normalized Mean Bias Factor (B_{NMBF})

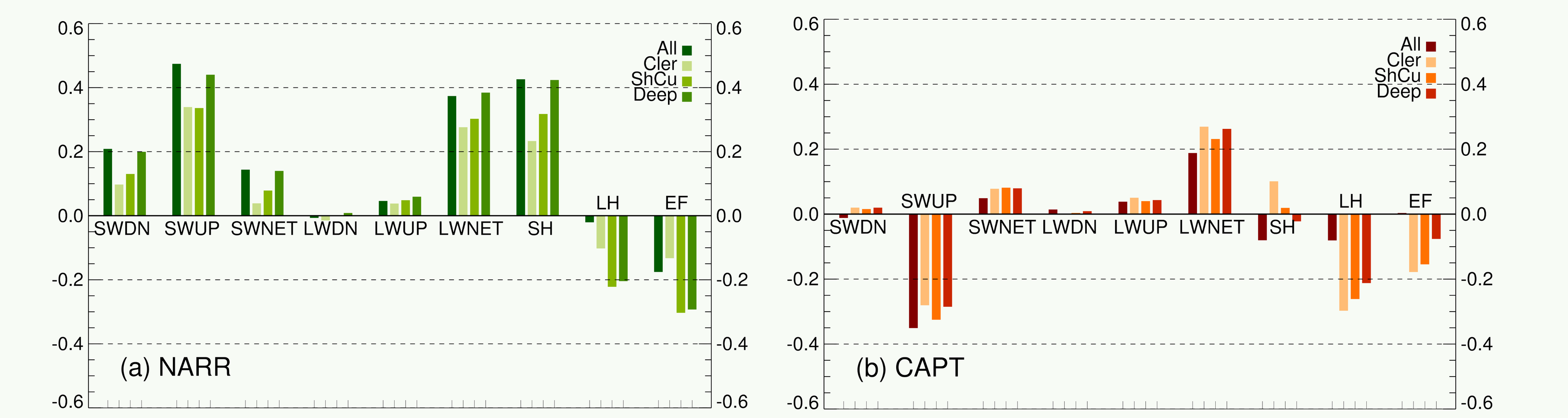

Fig. 2: B_{NMBF} of daily mean energy budget components for (a) NARR and (b) CAPT. If $B_{NMBF} > 0$, the model overestimates the observations by a factor of $B_{NMBF}+1$; if $B_{NMBF} < 0$, the model underestimates the observations by a factor of 1- B_{NMBF}.

Diurnal cycle of clouds and precipitation

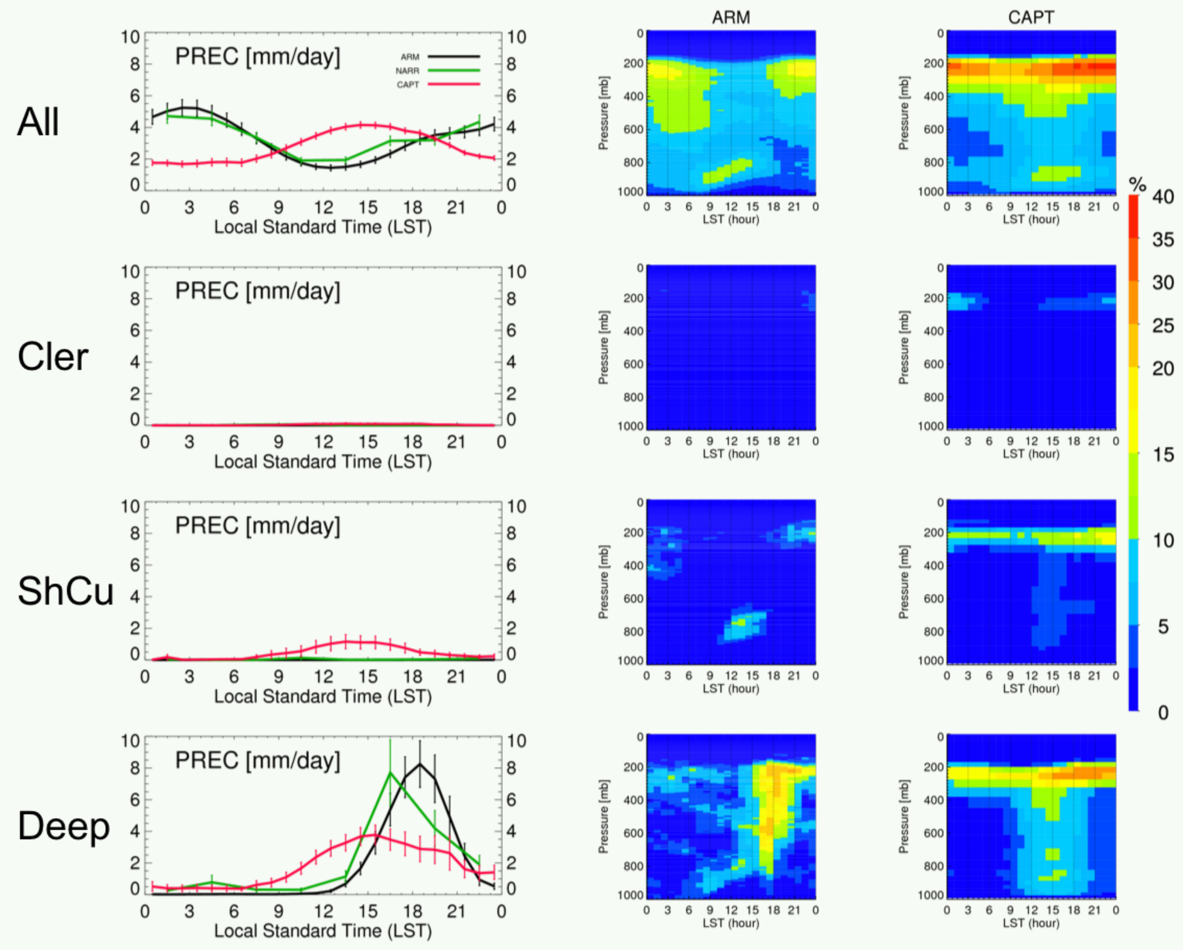

All (warm-season)

- Diurnal precip. peaks around noon
- Greater high-level clouds

Clear-sky regime

- Overall performance is pretty good

Shallow cumulus regime

- Precip. peaks ~ 1 mm/day
- Less low-level clouds, but more high-level clouds

Late-afternoon deep conv. regime

- Precip. starts earlier, but with a lower maximum rain rate
- No shallow-to-deep transition

Fig. 3: Diurnal cycle of (left) domain-average precipitation and (right) cloud fraction for different convection regimes.

"Correct" and "Wrong" cases in CAPT

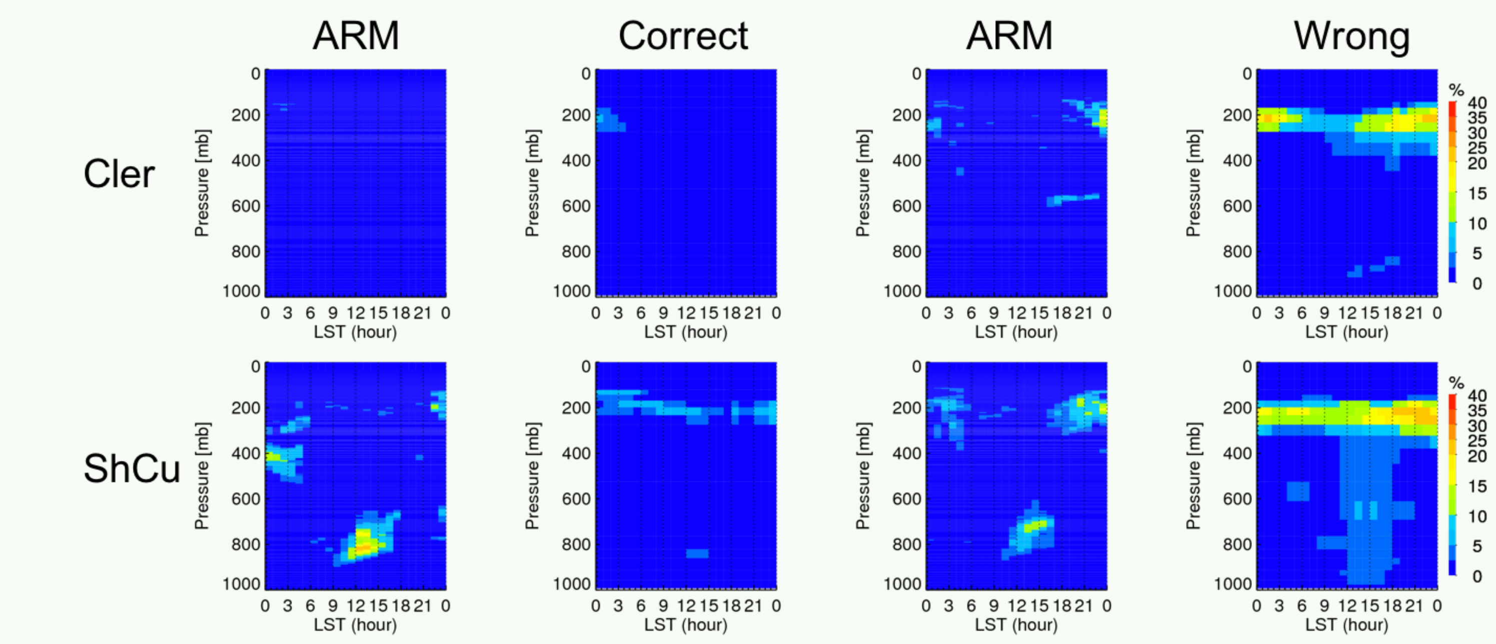

Fig. 4: Diurnal cycle of vertical profiles of cloud fraction in clear-sky and ShCu regime. "Correct" and "wrong" cases in CAPT are separated.

Clear-sky regime

- 49 out of 66 days (74%) are identified as clear-sky regime in CAPT model simulations
- "Wrong" cases are mainly attributed to days with daytime precip., where the ZM-scheme is triggered

ShCu regime

- 16 out of 48 days (33%) are identified as shallow cumulus regime in CAPT model simulations
- "Wrong" cases are mainly attributed to:
  1) days with daytime precip., where the ZM-scheme is triggered (14 days)
  2) days that are clear-sky regime (13 days)

Clear-sky Regime

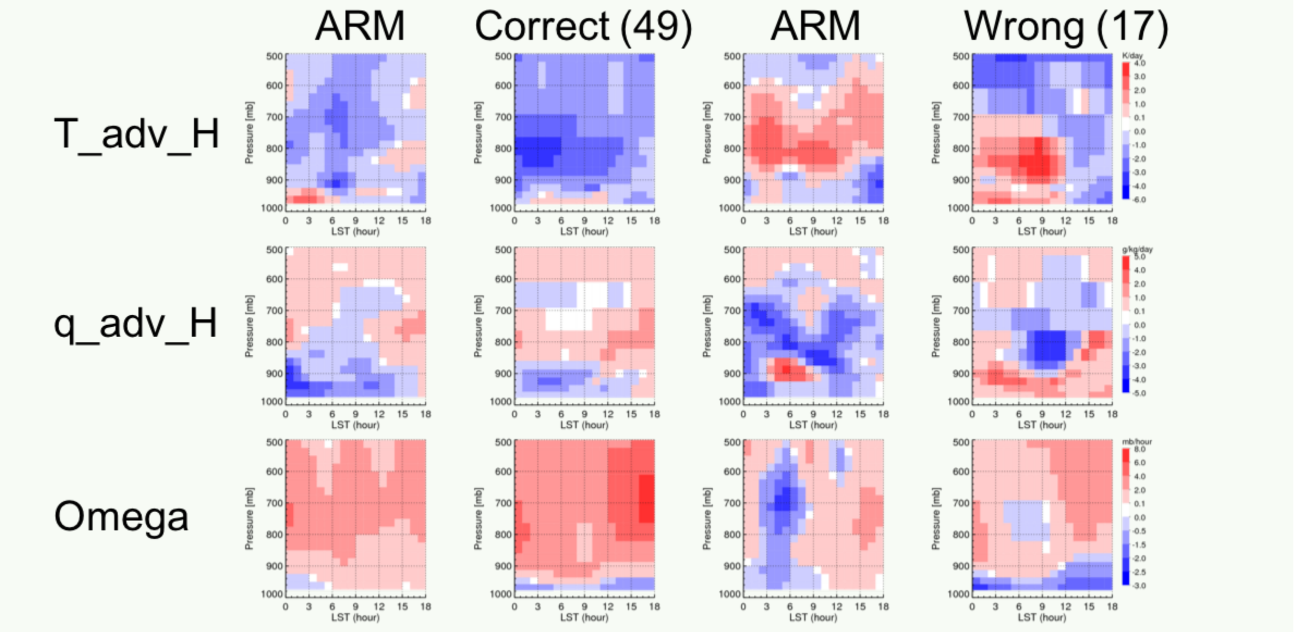

Fig. 5: Diurnal cycle of large-scale forcing for "correct" and "wrong" cases in CAPT. The corresponding large-scale forcing from ARM continuous forcing data in the same days are also shown.

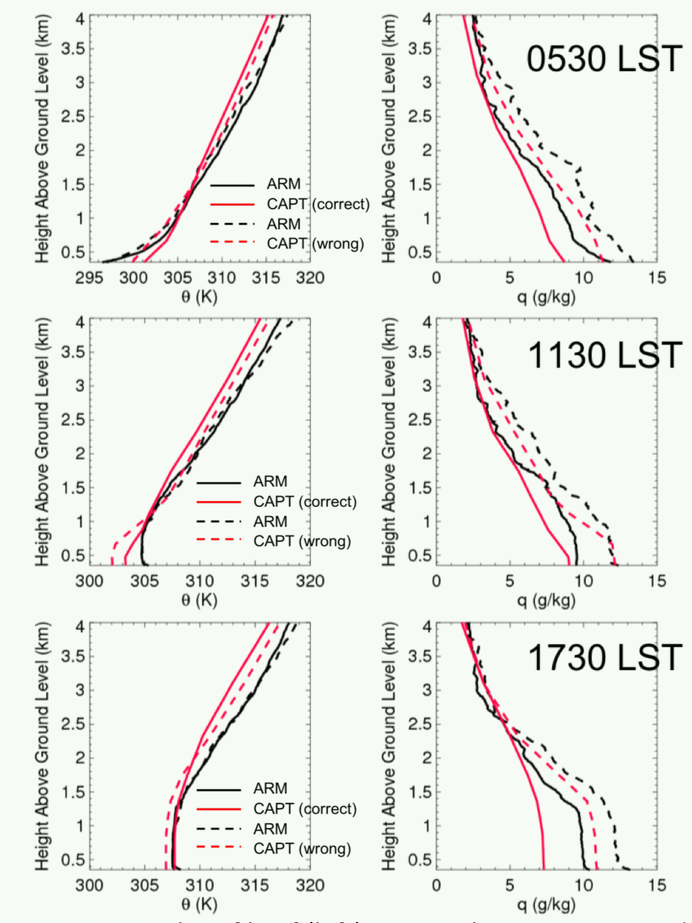

Fig. 6: Vertical profile of (left) potential temperature and (right) mixing ratio at 0530, 1130 and 1730 local time.

"Wrong" cases in CAPT

- Tend to occur on days when there is a warming and moistening in the early morning.
- Much more moisture at the near surface.

"Correct" cases in CAPT

- The development of convective boundary layer is much slower.
- The strength of L-A coupling is significantly stronger.

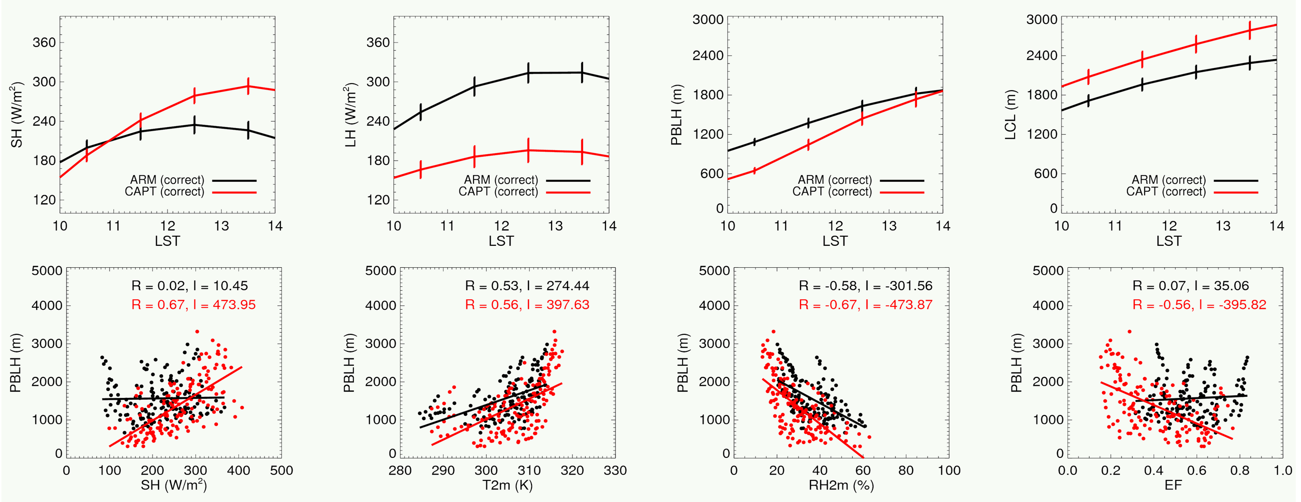

Fig. 7: (Top) Variation of SH, LH, PBL and LCL for "correct" cases in CAPT (between 10-14 LST only). (Bot.) Scatterplot of PBLH vs. SH, T_{2m}, RH_{2m}, and EF. ARM and CAPT are shown in black and red, respectively.

Summary and Future work

NARR

- Overestimate the observations of shortwave upward radiation, longwave net radiation and surface sensible heat flux by a factor of 1.4, especially in the late-afternoon deep convection regime.

CAPT model simulation

"Correct" cases in clear-sky regime

- A much lower PBLH at 1130 LST → the growth of PBLH is slower
- PBLH is correlated with surface sensible heat flux and evaporative fraction → a much stronger L-A coupling strength

"Wrong" cases in clear-sky regime

- 13 out of 66 clear-sky days in CAPT simulations have daytime precipitation, where the ZM-scheme is triggered.
- A warming and moistening in the early morning is noted in these days, accompanied with more moisture at the near surface.

Future work

- The L-A coupling in local convection regimes will also be evaluated in the E3SM regional refined model (RRM), which is ~25 km horizontal resolution and 72 pressure levels).

The authors would like to acknowledge Department of Energy (DOE) and Early Career Research Program (ECRP) for supporting this study. The authors sincerely thank Drs. Shuaiqi Tang and Shaocheng Xie for the ARM continuous forcing data, Hsi-Yen Ma for CAPT model results, Qi Tang for E3SM RRM model results, and Virendra Ghate for providing the algorithm of Z_i retrieval from RWP data. This work is performed under the auspices of the U.S. DOE by Lawrence Livermore National Laboratory under Contract DE-AC52-07NA27344. LLNL-POST-776827.